The Redox Boundaries of Earth's Interior

Vincenzo Stagno[1] and Yingwei Fei[2]

An octahedral (7 mm edge) diamond on kimberlite (Kimberley mine, South Africa). Image: Michele Macrì, courtesy of University Museum of Earth Sciences of Sapienza University of Rome (Italy).

1811-5209/20/0016-0167$2.50 DOI: 10.2138/gselements.16.3.167

The interior of the Earth is an important reservoir for elements that are chemically bound in minerals, melts, and gases. Analyses of the proportions of redox-sensitive elements in ancient and contemporary natural rocks provide information on the temporal redox evolution of our planet. Natural inclusions trapped in diamonds, xenoliths, and erupted magmas provide unique windows into the redox conditions of the deep Earth, and reveal evidence for heterogeneities in the mantle's oxidation state. By examining the natural rock record, we assess how redox boundaries in the deep Earth have controlled elemental cycling and what effects these boundaries have had on the temporal and chemical evolution of oxygen fugacity in the Earth's interior and atmosphere.

Keywords: redox state, mantle xenoliths, diamond inclusions, oxygen fugacity, volatile cycle

INTRODUCTION

The Earth's interior represents the largest reservoir of volatile elements (e.g., carbon, hydrogen, sulfur, nitrogen, oxygen) in the planet. The migration of volatiles to the shallow portions of the planet and, eventually, out into the atmosphere, plays an important role in planetary evolution. This process is strongly controlled by physical and chemical conditions at depth. Oxygen fugacity (f_{O_2}), or the partial pressure of oxygen (pO_2) in the case of gaseous mixtures in the atmosphere or volcanic gases, is a critical thermodynamic variable that controls the presence and proportions of multiple oxidation states of an element in minerals, liquids, and gases.

The differentiation of metal and silicate that occurred in the interior of the proto-Earth following its accretion from the solar nebula (Righter et al. 2020 this issue) led to oxygen redistribution, resulting in a stratification of oxidation state by sinking of reduced iron (Fe^0) metal into the core and bonding of O^{2-} to mantle silicates, followed by outgassing of H_2O-vapor, CO_2, and CO into the atmosphere (Fig. 1). The Earth's early atmosphere contained almost no free oxygen (Fig. 2), and its composition was probably more similar to that of extremely reduced volcanic gases (pO_2 of 10^{-6} atm). The atmosphere has become increasingly oxidized over time, a phenomenon that has been plausibly linked to the dynamic changes undergone by Earth, including the initiation of plate tectonics, the formation of continents, and the appearance of life (Fig. 2) (see Reinhard and Planavsky 2020 this issue). A possible link between the redox state of the Earth's interior and its atmospheric composition has been a matter of investigation over the last few decades through laboratory experiments and geochemical analysis of natural rocks. The evolution of the mantle's oxidation state, at least locally, is strongly influenced by recycling of surface materials via subduction. We can investigate the mantle's redox state by determining the mineralogy and chemical compositions of the mantle rocks, as well as understanding the effect of pressure and temperature on element partitioning among the coexisting phases. The observed mineralogy and chemistry of planetary interiors represent the final integration of numerous geodynamic

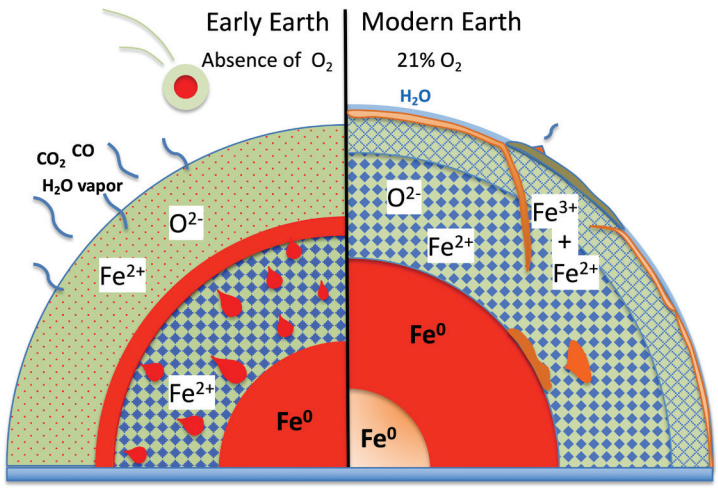

Figure 1 Schematic of the evolution of redox boundaries of the Earth's interior. (**Left**) Differentiation of the early Earth. Reduced metal (red teardrop shapes) sinks through the molten silicate to the core to establish oxidation state stratification between the mantle and the core at about 2 log units below the iron–wüstite, IW, buffer. (**Right**) The oxidation state of modern Earth's mantle has been significantly modified by subduction: heterogeneous f_{O_2} is expected in subduction zones. Layers shown are the inner core, outer core, lower mantle, upper mantle, and crust; oceanic crust (light orange) can subduct down to lower mantle depths. Note development of mantle plumes (orange) at the bottom of the lower mantle.

1 Sapienza University of Rome
Department of Earth Sciences
Rome, Italy
E-mail: vincenzo.stagno@uniroma1.it

2 Earth and Planets Laboratory
Carnegie Institution for Science
Washington DC, USA
E-mail: yfei@carnegiescience.edu

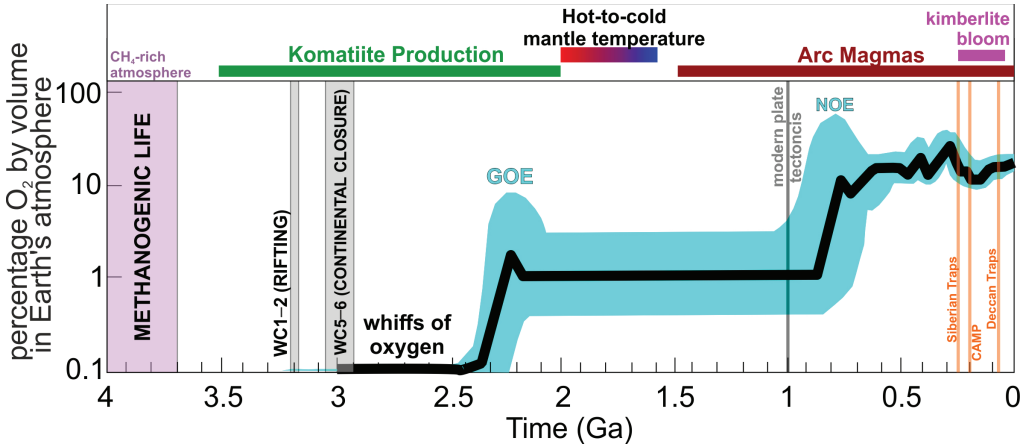

Figure 2 Variations in atmospheric oxygen partial pressure (pO_2) over the Earth's history. The maximum values are represented by the Great Oxidation Event (GOE) at 2.5–2.0 Ga and the Neoproterozoic Oxygenation Event (NOE) at 1.0–0.8 Ga. These two events are shown in relation to high-impact geological events such as the onset of plate tectonics through the Wilson Cycle (WC): WC1 and 2 for rifting, WC5–6 for continental collision (Shirey and Richardson 2011). These cycles are accompanied by the production of large volumes of magmas formed at hot mantle temperatures (producing komatiites) and cold mantle temperatures (as for arc magmas and kimberlites) (Tappe et al. 2018), plus the development of three large igneous provinces (LIPs): the Siberian Traps (predominantly Russia), the Central Atlantic Magmatic Province (CAMP), and the Deccan Traps of India. These LIPs likely caused mass extinctions (orange bars). The width of the blue band denotes uncertainty. The onset of modern plate tectonics is according to current continental growth models (Tappe et al. 2018). The timing of 'whiffs of oxygen' is marked by the enrichment of metals, such as Mo and Re, in the ocean resulting from their weathering-promoted mobilization from shallow sediments (after Lyons et al. 2014; see also Reinhard and Planavsky 2020 this issue).

processes dating back to the formation of the solar system: these processes involve planetary accretion, core–mantle separation, and plate tectonics. In order to address the nature of redox boundaries in the interior of a planet, we summarize the oxidation state recorded in natural mantle rocks, ancient and contemporary lavas, and preserved mineral inclusions in sublithospheric diamonds. These natural observations are combined with experimental studies aimed at simulating the Earth's interior to understand how the redox state has evolved over geological time.

Peridotites and eclogites are mantle-derived rocks whose minerals (chiefly olivine, orthopyroxene, clinopyroxene, spinel, and garnet) contain multivalent elements, such as iron, chromium, and vanadium. The ratios of the oxidized and reduced forms of these elements are sensitive to the redox conditions at which they formed. Incorporation of these elements in their oxidized or reduced form can be used to determine the f_{O_2}, which is taken as representative of the redox state of the mantle from which these rocks are derived. Mantle rocks from ancient Archaean cratons often host diamondiferous deposits, such as those in South Africa and Canada. Because carbon may exist either as oxidized carbonate (CO_3^{2-}) or reduced graphite/diamond (C^0), the presence of diamonds suggests that these mantle rocks equilibrated under reducing conditions. Two important goals in experimental geochemistry have been 1) to investigate how the behavior of relevant elements has been influenced by f_{O_2} and to develop interpretative models to understand the change of redox conditions in the Earth's interior, and 2) to explore how this might have controlled atmospheric composition though space and time. Because mantle rocks exposed at the surface are only those equilibrated up to, at most, depths of 200–250 km, information on the redox state of the upper mantle transition zone (410–660 km) and lower mantle (660–2,890 km) relies on the discovery and study of mineral inclusions in sublithospheric diamonds. In order to use inclusions composition to understand the redox conditions of the deep mantle, it is necessary to carry out experimental syntheses of phase equilibria and determine element partitioning under appropriate conditions. Analyses of data from natural rocks and laboratory experiments have allowed us to understand the extent to which the Earth's interior can be considered stratified, having either gradual or sharp redox boundaries. Here, we summarize our understanding of redox conditions and evolution in Earth's deep interior.

MANTLE OXIDATION STATE FROM THE STUDY OF NATURAL ROCKS AND ERUPTED LAVAS

The oxidation state of Earth's interior controls the speciation of multivalent elements, such as carbon (C^0 or C^{4+}) and iron (Fe^0, Fe^{2+}, or Fe^{3+}) in minerals and melts. The transformation from reduced phases such as carbide, graphite, and diamond, to oxidized carbonate minerals and melts provides an important indicator of mantle oxidation state. It also affects mantle processes due to changes in physicochemical properties, such as the melting of mantle rocks at lower temperatures by the addition of CO_2 (i.e., redox melting) (Stagno et al. 2013 and references therein). On the other hand, carbonate minerals and melts can be deprived of oxygen as a consequence of redox conditions buffered locally by the oxidation of Fe^{2+} to Fe^{3+} in minerals to form elemental carbon (Rohrbach and Schmidt 2011). The change of redox state of the mantle may play an important role in the recycling and mobilization of deep carbon and the production of a large spectrum of magmas at different depths over time (Stagno 2019).

The redox state of the continental lithospheric mantle has been investigated extensively through the analyses of natural rocks and the application of oxy-thermobarometers that use mineral equilibria to estimate their redox state through the correlation between the $Fe^{3+}/\sum Fe$ ratio of minerals and f_{O_2} (Frost and McCammon 2008). The $Fe^{3+}/\sum Fe$ ratio is typically measured by Mössbauer spectroscopy or is estimated on the basis of charge balance calculations. Thermodynamic calculations supported by experiments have facilitated the use of three important mineral equilibria as oxy-thermobarometers for spinel- and garnet-peridotites and for eclogites (Stagno 2019). Figure 3 plots the measured f_{O_2} of natural mantle rocks, normalized to a common reference buffer, in this case fayalite–magnetite–quartz (FMQ). The results show a heterogeneous mantle oxidation state, varying by 7 log units over 250 km depth. The general trend becomes more reduced with depth as result of the positive pressure effect on the incorporation of Fe^{3+} in garnet's crystal structure. Deep mantle eclogites (>175 km) can extend to the reduced conditions required to stabilise metallic Fe and methane-rich fluids, as indicated by the dot-dashed and dotted lines in Figure 3.

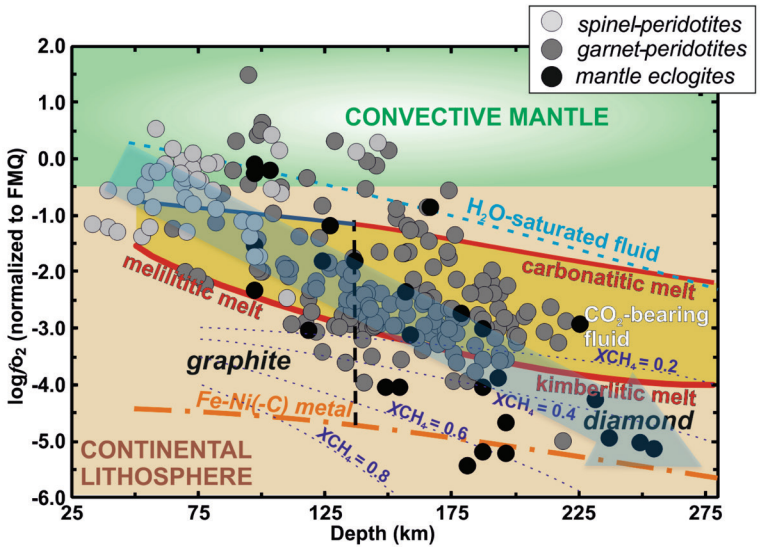

Figure 3 Plot of logf_{O_2} (relative to the fayalite–magnetite–quartz, FMQ, buffer) as a function of depth. Grey/black circles represent the calculated values for mantle peridotite and eclogite xenoliths using spinel and garnet oxy-thermobarometers (Stagno 2019). The thick light-blue arrow (going upper left to lower right) indicates the general trend of upper mantle redox state. The red lines are oxygen fugacities calculated along a cratonic geotherm of 44 mW·m^{-2} that define the stability field for diamond (or graphite) coexisting with solid (liquid) carbonate and kimberlitic magmas, respectively. The vertical dashed line represents the graphite–diamond boundary. The orange line is the Fe–Ni precipitation curve (Frost and McCammon 2008). In addition, the light and dark blue lines represent the calculated f_{O_2} at which C–O–H fluids in equilibrium with graphite/diamond consist of pure water (H_2O maximum) or the mole fractions of methane (XCH_4 = 0.2, 0.4, 0.6, and 0.8) according to Luth et al. (2014). The green and brown boxes mark the convective mantle and continental lithosphere, respectively.

Figure 3 also shows the calculated f_{O_2} as a function of depth for C–O–H fluids of different compositions that are in equilibrium with graphite/diamond, marked by the mole fractions of methane (XCH_4) (dark blue lines). The observations show that peridotites and eclogites can coexist with C–O–H fluids along cratonic *P*–*T* conditions. Under more oxidized conditions, H_2O-saturated fluids coexist with mantle rocks (blue dashed line), the fluids then becoming progressively richer in C as f_{O_2} decreases. The formation of rare carbonate-rich magmas, such as carbonatites and kimberlites, is the consequence of the oxidation of elemental carbon to CO_2 (yellow area) that, in turn, lowers the melting temperatures of peridotite (or eclogite) rocks at depth (Hammouda and Keshav 2015). Under more reducing conditions, partial melting of peridotite is inhibited by the presence of coexisting (nonreactive) methane-bearing fluids. Interestingly, most mantle rocks fall in the diamond and graphite stability fields, while thermodynamic models predict the potential coexistence of small volumes of water, CO_2(–H_2O)-rich magmas (and/or fluids), and methane, probably involving the following redox equilibria:

$$2Fe_2O_{3(solid)} + C = 4FeO_{(solid)} + CO_{2(vapor/melt)} \quad (1)$$

$$Fe_2O_{3(solid)} + H_2 = 2FeO_{(solid)} + H_2O_{(vapor/melt)} \quad (2)$$

$$2Fe_2O_{3(solid)} + CH_4 = 4FeO_{(solid)} + C + 2H_2O_{(vapor/melt)} \quad (3)$$

For these reactions, $Fe_2O_{3(solid)}$ and $FeO_{(solid)}$ refer to ferric and ferrous iron incorporated in upper mantle minerals, predominantly spinel and garnet. Importantly, the reactions shown in Equations (1) and (3) are those causing mantle redox melting to produce a wide range of CO_2- and H_2O-bearing magmas until all volatiles are exhausted, whereupon f_{O_2} is solely buffered by the coexisting minerals. Such magmas are rarely observed in nature. On the other hand, the reaction in Equation (2) is likely to have occurred in the interior of Earth after core formation where the release of H_2 brought about rapid oxygenation of the residual early formed mantle and an enrichment in water. Conversely, in subduction-related environments, the reactions in Equations (1)–(3) are probably controlled by locally released decarbonation and/or dehydration reactions in the subducted slab (Frost and McCammon 2008; Debret and Sverjensky 2017).

Because most of the rocks plotted in Figure 3 are of Archaean age, knowledge of their f_{O_2} permits understanding of how mantle redox state has changed over time. Three main points remain a matter of debate. (1) Does the f_{O_2} gradient observed in peridotites from the continental lithosphere hold for the convective (asthenospheric) mantle? (2) Do erupted magmas inherit the oxidation state of their mantle source rocks? (3) Has mantle redox state changed gradually over time? Answers to these questions are related to the redox boundaries in the interior of Earth. The most fertile garnet peridotite rocks [e.g., peridotite xenolith sample PHN1611 from Lesotho, see McCammon and Frost (2008)] have a bulk chemistry that coincides with that inferred for bulk silicate Earth (BSE) on cosmochemical grounds. For this reason, it is a suitable analogue for the asthenospheric mantle. By assuming an $Fe^{3+}/\sum Fe$ equal to that found in abyssal peridotites (1%–3%), thermodynamic models (Stagno et al. 2013; Stagno 2019) predict a similar redox profile to that observed for the continental lithosphere (Fig. 3) with f_{O_2} as low as –5 log units (ΔFMQ) at depths greater than 175 km.

Geochemical data (CO_2 vs Nb and CO_2 vs Ba) in oceanic basalts have been recently used (Eguchi and Dasgupta 2018) to argue that more oxidizing conditions, between –0.5 and +2 log units (ΔFMQ), must exist in the mid- to deep-oceanic mantle down to ~150 km in depth. This is due to the requirement that carbon must be mobilized from the subducted slab in the form of CO_2, thereby producing the observed enrichments in erupted lavas. Interestingly, the chemical composition (SiO_2/CO_2 ratio) of small-degree partial melts is determined by the depth, mantle temperature, and local mantle f_{O_2} at which elemental carbon is oxidized to carbonate by the redox reaction shown in Equation (1). These magmas undergo devolatilization, changes in melt polymerization, crustal assimilation, fractional crystallization, and net oxidation during their ascent toward the surface. Once the magmas are exposed at the surface, alteration processes can mask their initial redox state and make it difficult to link them to the f_{O_2} of the source. The effect of devolatilization on the residual melt has been attested to by the change in oxidation state of iron and sulfur in droplets of basaltic magmas (as melt inclusions) trapped in olivine from Kilauea volcano (Hawaii, USA) (Moussallam et al. 2016) and Laki volcano (Iceland) (Hartley et al. 2017) relative to their respective host magmas. The loss of volatile elements (e.g., sulfur and H_2O) would lead to a reduction of the erupted lavas compared to the preserved un-degassed magmas through the following reaction:

$$H_2S_{(melt)} + 3Fe_2O_{3(melt)} = SO_{2(vapor)} + 6FeO_{(melt)} + H_2O_{(vapor)} \quad (4)$$

Birner et al. (2018) showed agreement between the f_{O_2} of mid-ocean ridge (MOR) basalts and that of the corresponding MOR peridotites when both are back-calculated to source *P*–*T* conditions. However, the spread in f_{O_2} values in MOR basalts and peridotites have distinct standard deviations, with MOR basalts being more homogeneous than the peridotites. Indeed, heterogeneities are observed even at the hand-specimen scale. These discrepancies were also reported in experimental studies aimed at reproducing melting conditions of a fertile spinel peridotite (Sorbadere et al. 2018). Further studies are needed to better understand how the signature of mantle redox state is physically transferred from rocks to partial melts and, in turn, to magmatic gases that ultimately are released to the atmosphere.

REDOX STATE OF THE TRANSITION ZONE AND LOWER MANTLE FROM INCLUSIONS IN SUPERDEEP DIAMONDS

Mantle xenoliths provide a unique window on the redox state of the upper mantle down to ~250 km. We have a reasonably good understanding of redox variations with depth and the key factors that control those variations, as illustrated in Figure 3. However, information on even deeper portions of the upper mantle, the transition zone (410–660 km) and the lower mantle (down to ~2,890 km), is limited because only a few, rare diamond inclusions have been found from those depths. These sublithospheric (or superdeep) diamonds are witness to geological processes occurring in the hidden deep mantle (Kaminsky 2012). Minerals found in superdeep diamonds include majoritic garnet, carbonates, ringwoodite, $CaSiO_3$ walstromite, ferropericlase, Fe–Ni alloys, and carbides. Analyses of those inclusions, supported by experimental petrology studies, allows inferences to be made as to the possible deep mantle *P*–*T*–f_{O_2} conditions at which the inclusions formed. Such information is particularly valuable in the case of minerals formed prior to entrapment by the growing diamonds (i.e., protogenetic inclusions). To date, the redox state of the deep mantle has been determined for a suite of diamonds from Jagersfontein (South Africa) using the Fe^{3+} content of majoritic garnet inclusions that equilibrated at depths of 220–550 km (Kiseeva et al. 2018). In addition, some 53 Type II diamonds contained metallic inclusions along with H_2 fluids. These diamonds are interpreted to have formed in the transition zone by precipitation from an Fe–Ni liquid metal (Smith et al. 2016). However, some deep diamonds show inclusions of solid carbonates (Kaminsky 2012 and references therein), suggesting some portions of the lower mantle might be oxidized to similar levels as the upper mantle.

Figure 4 shows the estimated f_{O_2} from different deep diamond inclusions and provides a snapshot of the different oxygenation levels of the mantle at different depths. Experimental measurements of the f_{O_2} at which diamonds and solid carbonate can coexist along with silicate minerals of the transition zone and lower mantle (see Stagno 2019 and references therein) suggest a general trend of decreasing f_{O_2} with depth in the deep mantle (the dark blue line on Fig. 4). The relationship can be applied as oxybarometers for carbonate inclusions trapped in superdeep diamonds. For comparison, the upper mantle redox state (gray shaded region below 10 GPa on Fig. 4) recorded by mantle xenoliths has a much steeper pressure dependence (cf. Fig. 3); the likely f_{O_2} of the transition zone and lower mantle (the horizonal gray shaded region on Fig. 4) would be close to the iron–wüstite (IW) buffer. The estimated f_{O_2} of mantle-derived rocks and diamond inclusions provides a more complex picture of the deep mantle. Majoritic garnet inclusions from Jagersfontein (red diamond symbol) show

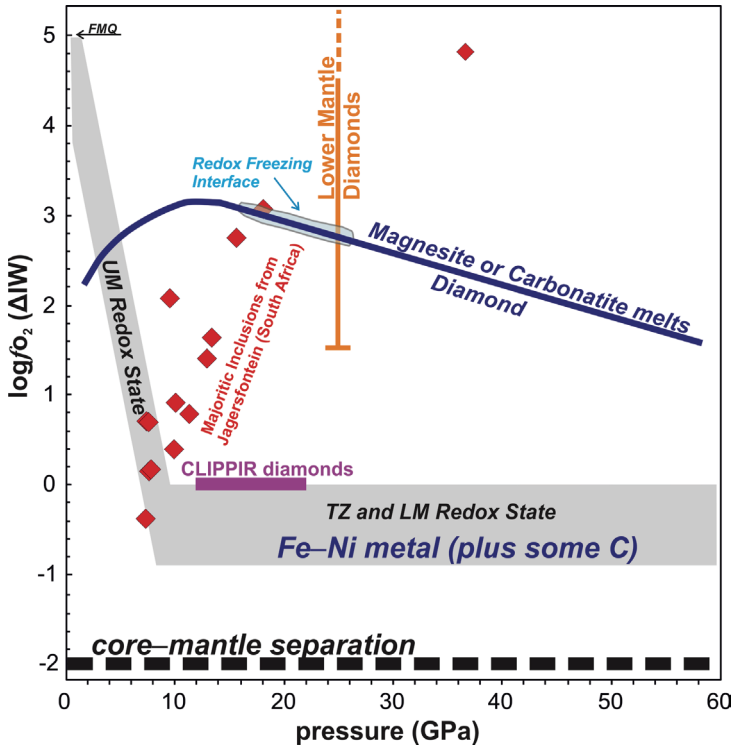

Figure 4 Plot of logf_{O_2} (relative to changes in the iron–wüstite, IW, buffer) as a function of pressure in the deep mantle. The red diamond symbols show the estimated f_{O_2} from majorite inclusions in diamonds (Kiseeva et al. 2018); the thick purple line shows the estimated f_{O_2} from metal-bearing "CLIPPIR" (Cullinan-like, large, inclusion-poor, pure, irregular, resorbed) diamonds (Smith et al. 2016); the vertical orange line shows the estimated f_{O_2} from ferropericlase inclusions in diamonds (Kaminsky et al. 2015). The dark blue line indicates the f_{O_2} at which diamonds and carbonate (magnesite) are in equilibrium with a mantle mineral assemblage (Stagno 2019). The gray shaded region indicates the upper mantle (UM) redox state recorded by mantle xenoliths (cf. Fig. 3) and the likely f_{O_2} of the transition zone (TZ) and lower mantle (LM), if it is reduced enough to allow Fe–Ni alloy (± dissolved carbon) to be stable (Frost and McCammon 2008). Most of the superdeep diamonds are thought to have originated at the interface between the oxidized subducting slab and the reduced asthenospheric mantle (shaded blue) where CO_2-rich fluids have been proposed to "freeze" (Rohrbach and Schmidt 2011).

a large range of f_{O_2}, whereas CLIPPIR (Cullinan-like, large, inclusion-poor, pure, irregular and resorbed) diamonds (purple line) indicate very reducing conditions to help produce Fe–Ni metal alloy inclusions (Fig. 4). Indeed, the recovered inclusions and their redox conditions may reflect only local environments and may not be applicable to the whole mantle. The chemical compositions of natural mantle-derived rocks attest to the fact that the mantle's physical evolution through time has created chemical and f_{O_2} heterogeneities. The dichotomy between *sharp* versus *gradual* redox boundaries in Earth's interior is a result of mantle evolution and material exchange between the surface and deep mantle over time.

TEMPORAL VARIATIONS IN MANTLE f_{O_2}: GRADUAL VS SHARP BOUNDARIES

Whether mantle oxidation state has changed gradually or suddenly over time has long been debated. The temporal evolution of mantle redox state and that of melts and volcanic gases derived therefrom may have played a key role in the volatile cycle, greenhouse effects, plate tectonics, and life on Earth. To answer this question, geologists have been looking at potential geochemical markers in ancient rocks

and minerals. Redox-sensitive geochemical signatures, such as the cerium (Ce) concentration of Hadaean zircons and the vanadium/scandium (V/Sc) ratio of erupted basalts, have been used to claim the constancy of the mantle redox state over the last 3.8 billion years to values where carbon is stable as C^{4+} (i.e., CO_2 in solids, melts, and gases). In particular, the higher solubility of Ce^{4+} compared to Ce^{3+} in zircons equilibrated with melts allows an estimation of the oxidation state of Hadean melts with respect to MOR lavas (Trail et al. 2011). In addition, the V/Sc ratio in basaltic melts is a function of redox conditions during melting processes, with V^{5+} being more incompatible than Sc^{3+} at high f_{O_2} (Li and Lee 2004).

The investigation and quantification of mantle redox state over time requires the integration of f_{O_2} values, as estimated by oxy-thermobarometry, with radiometric dating of mantle rocks, inclusions in diamonds, and mantle-derived lavas. Figure 5 shows the temporal evolution of mantle f_{O_2} from the value set by core–mantle separation (IW–2, corresponding to FMQ–6) soon after Earth's accretion, to the ~IW+3.5 (FMQ–0.5) recorded by present-day mantle rocks. Figure 5 also shows a schematic model that takes into account gradual mantle self-oxidation (up to IW+2) caused by disproportionation of FeO to metallic Fe and Fe_2O_3 in the magma ocean (Armstrong et al. 2019). The model is constrained by f_{O_2} estimates of eclogitic, picritic, and komatiitic rocks of Archaean age, along with a determination of the mantle's oxidation state through Ce in Hadean zircons and oxy-thermobarometry of mantle rocks. For comparison, the redox state of present-day volcanic gases is also shown on Figure 5 (Moussallam et al. 2019). When these data are compared with modern MOR lavas, a gradual increase in f_{O_2} of the Earth's mantle can be seen in both komatiites (Nicklas et al. 2019) and eclogites (Aulbach and Stagno 2016). This conclusion contrasts with that of a previous geochemical model in which mantle oxygenation was inferred to have occurred suddenly based on f_{O_2} recorded by Hadean zircons (Li and Lee 2004; Trail et al. 2011). It is currently uncertain whether the scattered Hadean zircon data might refer to either local evidence of an already oxidized shallow mantle or the input of reduced chondritic material delivered during the Late Heavy Bombardment (about 4.1–3.8 Ga). The low redox state of Archean magmas implies low $Fe^{3+}/\sum Fe$ of the mantle source they were equilibrated with. Oxidized mantle sources are likely to turn elemental carbon and methane into the CO_2 and H_2O that are responsible for the formation of low degree partial melts (see Equations 1–3). For reduced mantle rocks, such as those in the hot Paleoarchaean, volatiles were likely stored in their elemental state or dissolved in metallic phases. If any volcanic outgassing occurred, this must have been characterized by a redox state 2–3 orders of magnitude lower than present.

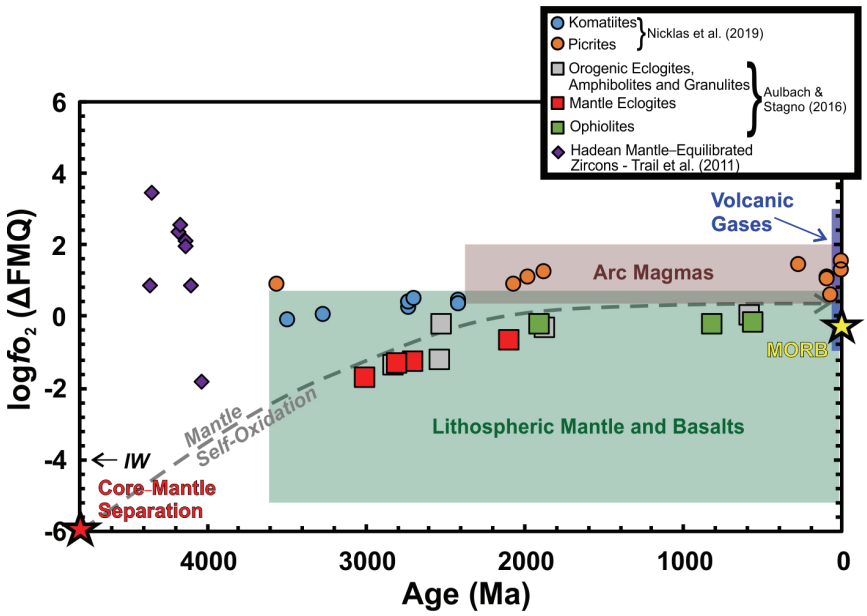

Figure 5 Temporal variation of $\log f_{O_2}$ (relative to changes in the fayalite–magnetite–quartz, FMQ, buffer) from the Earth's formation to the present-day; the iron–wüstite, IW, buffer is indicated at –4. The f_{O_2} values were estimated from the chemical reconstruction of V/Sc ratios of Archean metabasalts (Aulbach and Stagno 2016), V partitioning between olivine and melt for picritic and komatiitic rocks of Archaean age (Nicklas et al. 2019), and Ce concentration in Hadean zircons (Trail et al. 2011). The f_{O_2} of present mid ocean ridge basalt (MORB) is after Berry et al. (2018). The dashed line is the idealized trend if self-oxidation occurred during magma ocean crystallization gradually through time due to secular cooling. The estimated uncertainties in the calculated f_{O_2} values are generally within ±0.5 log units. The f_{O_2} interval recorded by natural rocks and gases is shown, for comparison, by the shaded areas.

THE REDOX STATE OF THE SUBDUCTED SLAB AND VOLATILE SPECIATION

The subducted slab, as the main carrier of oxidized fluids such as water and CO_2, is generally believed to be responsible for oxygenation of the mantle. The slab's diverse mineral assemblages, developed from the many metamorphic reactions at the different depth and temperature regimes experienced by the downgoing slab, have resulted in gross changes in the mantle from it being oxidized (FMQ+2) to being reduced f_{O_2} (FMQ–1) (Frost and McCammon 2008). This, in turn, influences the transport and oxidation state of the volatile elements at depth, such as H, C, and S, which are the dominant gases released from arc volcanoes upon eruption. A key role is played by the subduction of hydrous phases in the subducted lithospheric mantle, such as serpentinites. Subducted serpentinites show f_{O_2} varying between FMQ–2 and FMQ–1 (Deschamps et al. 2013). Observations from natural rocks, such as those exposed in the Cerro del Almirez Massif (Spain) and which are representative of serpentinized oceanic lithosphere, show, however, that the redox state of serpentinites might be more heterogeneous depending on the initial bulk composition. In particular, the presence of either sulfide or Fe–Ni metal alloys is able to buffer the local f_{O_2} at reduced values of –5 log units below FMQ (Debret and Sverjensky 2017), thereby stabilizing H_2 and CH_4 in equilibrium with serpentinites. In the absence of reduced phases, on the other hand, and as prograde metamorphism increases, the buffering capacity diminishes from abyssal serpentinites to chlorite harzburgites as a consequence of decreasing the bulk $Fe^{3+}/\sum Fe$ in the rock from ~70% to ~35% due to antigorite breakdown (at a depth of ~50 km and ~650 °C). As a breakdown product, Fe^{2+}-rich minerals such as olivine and orthopyroxene form along with less Fe^{3+}-rich chlorite plus water according to the reaction shown in Equation (2) (Debret and Sverjensky 2017 and references therein). This, in turn, favors the circulation of oxidized fluids, such as H_2O, and sulfates at f_{O_2} values between –1 and +5 log units below FMQ.

In contrast with the subducted ultramafic, serpentine-bearing portion of the slab, metamorphism of the subducted oceanic crust gives rise to a mineral assemblage containing Fe-bearing eclogitic phases, such as omphacitic clinopyroxene and garnet. Both minerals have a large capacity for incorporating Fe^{3+}. With increasing depth, the silicates could incorporate increasing amounts of Fe^{3+} while simultaneously reducing the volatile species. This form of oxygen sequestration by minerals would cause the reduced portions of the subducted slab to host diamond as the stable form of carbon (cf. FIG. 3) (Stagno 2019). Reduced C–O–H fluids with methane and light hydrocarbons would form at the expense of subducted carbonates at depths of 200–400 km. Recently, the interface between subducted slab and asthenospheric mantle has been described as favorable for the formation of diamonds due to the presence of chemical and f_{O_2} gradients (Thompson et al. 2016). Only when portions of the slab enter the convective mantle, can the Fe^{3+} of silicates be reduced back to Fe^{2+} due to the effect of pressure on the reaction in Equation (1), providing enough oxygen to reconvert C to CO_2 and then lower the melting temperature of the surrounding rocks to produce CO_2- and H_2O-bearing magmas and metasomatic fluids.

In summary, the current redox state of the Earth's interior results from initial differentiation on a global scale, modified subsequently by exchange of materials between the interior and the surface at plate boundaries through time. By experimental simulations and analysis of natural samples, we can derive information on the mantle's redox state at different depths and its temporal evolution. Experimental studies, supported by observations, suggest that the redox boundaries in the Earth's interior are gradual rather than sharp because of mineral–mineral and mineral–fluid chemical interactions. The general trend is that the mantle has become progressively more oxidized through time, although the mantle's oxidation state remains spatially heterogeneous.

ACKNOWLEDGMENTS

VS acknowledges financial support from Sapienza University of Rome through "Bandi di Ateneo 2016–2018". YF acknowledges supports from NASA, NSF, and Carnegie Science. We thank Paolo Sossi and an anonymous reviewer for constructive suggestions.

REFERENCES

Armstrong K, Frost DJ, McCammon CA, Rubie DC, Boffa Ballaran T (2019) Deep magma ocean formation set the oxidation state of Earth's mantle. Science 365: 903-906

Aulbach S, Stagno V (2016) Evidence for a reducing Archean ambient mantle and its effects on the carbon cycle. Geology 44: 751-754

Berry AJ, Stewart GA, O'Neill HS, Mallmann GF, Mosselmans JF (2018) A re-assessment of the oxidation state of iron in MORB glasses. Earth and Planetary Science Letters 483: 114-123

Birner SK, Cottrell E, Warren JM, Kelley KA, Davis FA (2018) Peridotites and basalts reveal broad congruence between two independent records of mantle f_{O_2} despite local redox heterogeneity. Earth and Planetary Science Letters 494: 172-189

Debret B, Sverjensky DA (2017) Highly oxidising fluids generated during serpentinite breakdown in subduction zones. Scientific Reports 7, doi: 10.1038/s41598-017-09626-y

Deschamps F, Godard M, Guillot S, Hattori K (2013) Geochemistry of subduction zone serpentinites: a review. Lithos 178: 96-127

Eguchi J, Dasgupta R (2018) Redox state of the convective mantle from CO_2-trace element systematics of oceanic basalts. Geochemical Perspective Letter 8: 17-21

Frost DJ, McCammon CA (2008) The redox state of the Earth's mantle. Annual Review of Earth and Planetary Sciences 36: 389-420

Hammouda T, Keshav S (2015) Melting in the mantle in the presence of carbon: review of experiments and discussion on the origin of carbonatites. Chemical Geology 418: 171-188

Hartley ME, Shorttle O, Maclennan J, Moussallam Y, Edmonds M (2017) Olivine-hosted melt inclusions as an archive of redox heterogeneity in magmatic systems. Earth and Planetary Science Letters 479: 192-205

Kaminsky F (2012) Mineralogy of the lower mantle: a review of 'super-deep' mineral inclusions in diamond. Earth-Science Reviews 110: 127-147

Kaminsky FV and 6 coauthors (2015) Oxidation potential in the Earth's lower mantle as recorded from ferropericlase inclusions in diamond. Earth and Planetary Science Letters 417: 49-56

Kiseeva ES and 10 coauthors (2018) Oxidized iron in garnets from the mantle transition zone. Nature Geoscience 11: 144-147

Li Z-XA, Lee C-TA (2004) The constancy of upper mantle f_{O_2} through time inferred from V/Sc ratios in basalts. Earth Planetary Science Letters 228: 483-493

Luth RW, Stachel T (2014) The buffering capacity of lithospheric mantle: implications for diamond formation. Contributions to Mineralogy and Petrology 168, doi: 10.1007/s00410-014-1083-6

Lyons TW, Reinhard CT, Planavsky NJ (2014) The rise of oxygen in Earth's early ocean and atmosphere. Nature 506: 307-315

Moussallam Y and 6 coauthors (2016) The impact of degassing on the oxidation state of basaltic magmas: a case study of Kīlauea volcano. Earth and Planetary Science Letters 450: 317-325

Moussallam Y, Oppenheimer C, Scaillet B (2019) On the relationship between oxidation state and temperature of volcanic gas emissions. Earth and Planetary Science Letters 520: 260-267

Nicklas RW and 8 coauthors (2019) Secular mantle oxidation across the Archean-Proterozoic boundary: evidence from V partitioning in komatiites and picrites. Geochimica et Cosmochimica Acta 250: 49-75

Reinhard CT, Planavsky NJ (2020) Biogeochemical controls on the redox evolution of Earth's oceans and atmosphere. Elements 16: 191-196

Righter K, Herd CD, Boujibar A (2020) Redox processes in early Earth accretion and in terrestrial bodies. Elements 16: 161-166

Rohrbach A, Schmidt MW (2011) Redox freezing and melting in the Earth's deep mantle resulting from carbon–iron redox coupling. Nature 472: 209-212

Shirey SB, Richardson SH (2011) Start of the Wilson Cycle at 3 Ga shown by diamonds from subcontinental mantle. Science 333: 434-436

Smith EM and 6 coauthors (2016) Large gem diamonds from metallic liquid in Earth's deep mantle. Science 354: 1403-1405

Sorbadere F and 6 coauthors (2018) The behaviour of ferric iron during partial melting of peridotite. Geochimica et Cosmochimica Acta 239: 235-254

Stagno V (2019) Carbon, carbides, carbonates and carbonatitic melts in the Earth's interior. Journal of the Geological Society 176: 375-387

Stagno V, Ojwang DO, McCammon CA, Frost DJ (2013) The oxidation state of the mantle and the extraction of carbon from Earth's interior. Nature 493: 84-88

Tappe S, Smart K, Torsvik T, Massuyeau M, de Wit M (2018) Geodynamics of kimberlites on a cooling Earth: clues to plate tectonic evolution and deep volatile cycles. Earth and Planetary Science Letters 484: 1-14

Thomson AR, Walter MJ, Kohn SC, Brooker RA (2016) Slab melting as a barrier to deep carbon subduction. Nature 529: 76-79

Trail D, Watson EB, Tailby ND (2011) The oxidation state of Hadean magmas and implications for early Earth's atmosphere. Nature 480: 79-82